eXPRESS Polymer Letters Vol.5, No.1 (2011) 38–46
Available online at www.expresspolymlett.com
DOI: 10.3144/expresspolymlett.2011.5

Facile synthesis of superhydrophobic TiO_2/polystyrene core-shell microspheres

*Z. M. Chen, S. J. Pan, H. J. Yin, L. L. Zhang, E. C. Ou, Y. Q. Xiong, W. J. Xu**

Institute of Polymer Science and Engineering, College of Chemistry and Chemical Engineering, Hunan University, Changsha 410082, China

Received 7 July 2010; accepted in revised form 12 September 2010

Abstract. In this paper, core-shell TiO_2/polystyrene (TiO_2/PS) microspheres with superhydrophobic properties were prepared via a facile method. Our method needs neither special apparatus nor complicated chemical treatment. The whole process includes two steps: firstly, coupling agent was used to modify TiO_2 by sol-gel method; secondly, fabrication of TiO_2/PS dispersions was carried out via *in-situ* free-radical polymerization strategy. The component and structure of the TiO_2/PS particles were characterized by Fourier transform infrared (FTIR) spectroscopy, thermogravimetric analysis (TGA), field emission scanning electron microscope (FE-SEM) and transmission electron microscopy (TEM). The TiO_2 gel particles with average diameter of 1 μm exhibited irregular spherical shape and obvious aggregation. Compared with the TiO_2 particles, the resulting TiO_2/PS particulates showed regular spherical shape, better dispersion and bigger size. By directly depositing the resulted TiO_2/PS dispersion on a Cu foil, the coating showed superhydrophobic property which was reflected by the contact angle (CA) of water on the surface with high water adhesion. The apparent CA of water is 153.5±1.5°, suggesting that this composite possesses well superhydrophobicity.

Keywords: *adhesion, TiO_2/PS particles, sol-gel method, in-situ free-radical polymerization, superhydrophobicity*

1. Introduction

Recently, organic/inorganic composites have been received great interest due to their unique properties and possibility for numerous applications in modern technology [1–3], such as electroplating [4], biotechnology [5] and electrochemistry [6]. The core-shell sphere is one of the most attractive composite structure because of its amazing functions originating from the different composition of the core and shell materials. Currently a lot of methods are available to prepare organic-inorganic hybrid particles with core-shell structure, such as subsequent polymerization [7], emulsion polymerization [8], layer-by-layer (LBL) method [9] and sol-gel method [10]. Among these methods, sol-gel process is undoubtedly one of the simplest and the cheapest techniques for the fabrication of materials starting from a chemical solution that reacts to produce colloidal particles.

In recent years, superhydrophobic surfaces, with a water CA greater than 150°, have received much attention not only for their significance to fundamental research but also for their important applications in fields ranging from self-cleaning materials to microfluidic devices [11, 12]. There exists two kinds of extremely superhydrophobic cases in nature, that is, 'sliding' superhydrophobic lotus leaves with ultralow water sliding resistance and 'sticky' superhydrophobic gecko feet with high adhesive force. Generally, micrometer or nanometer order rough surfaces with low-surface-energy materials are the keys to obtain superhydrophobic surfaces [13]. The materials having low surface energy used to make the superhydrophobic surfaces

*Corresponding author, e-mail: weijianxu59@gmail.com

are fluorocarbon, silicones, organic materials (polyethylene, polystyrene, etc.) [14], and inorganic materials (ZnO and TiO_2) [15]. There are many approaches to create rough surfaces, such as layer-by-layer and colloidal assembly [16, 17], laser/plasma/chemical etching [18–20], sol-gel processing [21–26], etc. Unfortunately, in many cases, the reported approaches employ either expensive materials, such as carbon nanotubes [27] and semi- or perfluorinated materials [28, 29], or multistep processes [23], thereby the applications in large-scale superhydrophobic surfaces are greatly hampered.

In our laboratory, click chemistry has been used to prepare cactus-like superhydrophobic surfaces with the water CAs greater than 150° [30]. In this paper, we choose TiO_2 and styrene as raw materials, which are of low-surface-energy. Because of TiO_2 gels are inorganic materials, but styrene is an organic material, therefore, the compatibility of them is not very good. 3-(trimethoxysilyl)propylmethacrylate (MPS) is indeed a good coupling agent to modify inorganic particles. Furthermore, the end group of MPS is C=C, when MPS hydrolyzed and grafted to TiO_2 gels, the C=C group can be reacted with styrene through *in-situ* polymerization. Firstly, MPS-TiO_2 gels are obtained via sol-gel method. Afterwards, TiO_2/PS dispersions were fabricated via *in-situ* free-radical polymerization. Finally, TiO_2/PS core-shell composites with superhydrophobic properties were prepared. By directly depositing the dispersion onto the substrate, a superhydrophobic (CA = 153.5±1.5°) and adhesive surface is obtained. Our strategy possesses various advantages: (1) the TiO_2/PS composites present superhydrophobic properties with high water adhesion, which have many potential applications, such as no loss microdroplet transfer, trace-liquid reactors, biochemical separation and *in-situ* detection [12, 31, 32]; (2) the raw materials of TiO_2 and styrene are pretty cheap, making the whole reaction cost-effective; (3) the whole reaction involves only two steps, which makes the synthetic process more facile, therefore, it is possible to introduce it into industry applications; (4) the as-prepared hybrids show excellent chemical and optical stability for there is no change of the water CAs of the coatings when exposing to UV light. It is expected that the facile and scalable synthesis of such robust uniform TiO_2/PS hybrids would pave the way for applying materials with superhydrophobic properties in practical fields.

2. Experimental

2.1. Materials

The coupling agent, 3-(trimethoxysilyl)propylmethacrylate (MPS), was received from Qufu Wanda Chemical Co., Ltd (Shandong, China). Ammonia (25–28 wt%), ethanol, 2,2-azobis(isobutyronitrile) (AIBN), N,N′-dimethylformamide (DMF) and styrene monomer were commercially available from Tianjin Damao Chemical Reagent Company (Tianjin, China). 2,2-azobis(isobutyronitrile) (AIBN) was recrystallized from tetrahydrofuran before use. The styrene monomer was distilled under reduced pressure to remove the inhibitor before polymerization, which was also received from Tianjin Damao Chemical Reagent Company (Tianjin, China). Tetrabutyl titanate (TBT) as the titania source was purchased from China Medicine Group Shanghai Chemical Reagent Company (Shanghai, China).

2.2. Synthesis of MPS-TiO_2 gels

Typically, MPS-grafted colloidal titanium gels were fabricated by the following steps: firstly, TBT (10 g) and MPS (0.73 g) in DMF ([TBT]:[MPS] = 10:1 mol/mol) were mixed in a round-bottom flask followed by stirring the mixture for 4 h until it was homogeneous. Then, the reaction of the mixture stirred at 60°C for 5 h after adding deionized water and little hydrochloric acid solution (36 wt%) ([TBT]:[H_2O]:[DMF] = 1:6:4 mol/mol). Finally, the MPS-grafted colloidal titanium suspensions were obtained, which was then filtered and washed by DMF, and finally the product was dried in vacuum.

2.3. Synthesis of TiO_2/PS microspheres

Subsequently, the TiO_2/PS composites were prepared via *in-situ* free-radical polymerization. The method for synthesis of TiO_2/PS microparticles is described briefly as follows: styrene monomer (20 g), AIBN (0.09 g), and DMF (50 ml) containing 0.2 g of MPS-grafted titanium gels were mixed in a round-bottom flask at room temperature for 30 min. The mixtures were then reacted at 68°C for 5 h under a nitrogen-protected atmosphere. Figure 1 shows the schematic synthesis route for TiO_2/PS microspheres. The fabrication of PS spheres is the

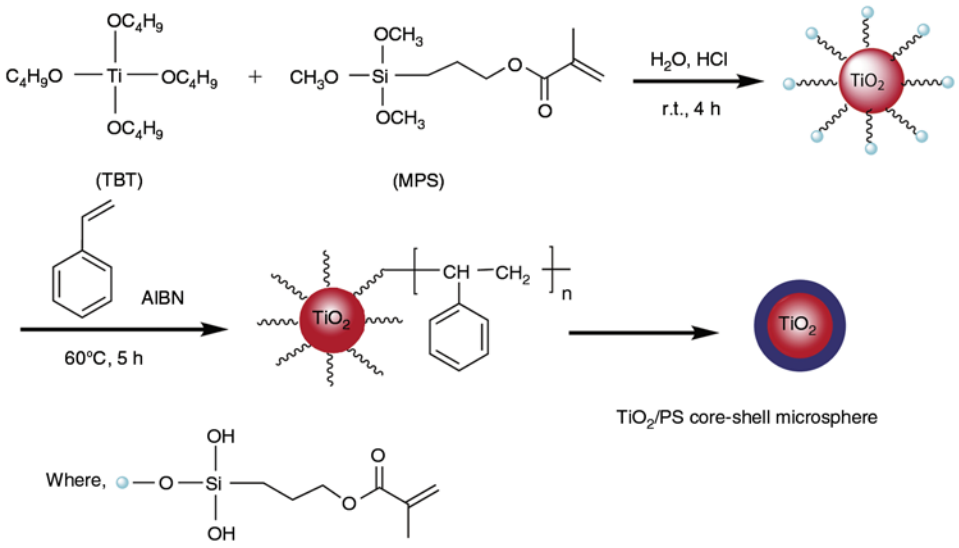

Figure 1. Synthesis route of TiO_2/PS core-shell materials from MPS modified TBT

same as the procedure of fabricating TiO_2/PS under the similar conditions without the addition of MPS-grafted titanium gels.

2.4. Preparation of superhydrophobic coatings

Copper foils (20 mm×10 mm×0.1 mm) were mechanically polished with a series of emery papers of different grit size (800, 2000) followed by rinsing in deionized water; they were ultrasonically cleaned in acetone and ethanol for 5 min, respectively. Then the as-prepared TiO_2/PS dispersions were coated on a clean copper foil and dried at room temperature for one day.

2.5. Characterization

Fourier transform infrared spectrometry (FTIR) was performed on a WQF-200 instrument (Rayleigh, Sci-Tek, Olney, UK) using conventional KBr pellets. Thermogravimetric analysis (TGA) was performed on a Netzsch STA409PC instrument (Netzsch, Selb, Germany) under a flowing argon atmosphere from 30 to 700°C at a scan rate of 10°C/min. Scanning electron microscope and energy dispersive X-ray spectra (SEM/EDX, JEOL, JSM-6700F) were used for the morphological and compositional analysis of the TiO_2/PS particles which was prepared on the substrate of copper foil. Transmission electron microscopy (TEM) images of the composites were obtained at 80 kV with a TEM-H800 (JEOL, Japan). The images of the air-solid-liquid interface were observed by an SONY microscope. The static water contact angles were measured with deionized water (4 μl) on a contact angle goniometer (JC2001) instrument at room temperature (about 28°C). The contact angles were measured at three different points for each sample surface, and the average values were reported here.

3. Results and discussion

3.1. Fabrication of TiO_2/PS microspheres

Figure 2 shows the FTIR spectrum of pristine MPS (a), MPS-TiO_2 particles (b), and TiO_2/PS microspheres (c). In Figure 2b corresponding to the TiO_2-MPS sample, the characteristic absorptions (cm^{-1}) of 2973–2928 (υ_{C-H}) and 1708 ($\upsilon_{C=O}$) for MPS are observed, which indicates that a few MPS molecules have been grafted on the TiO_2 particles suc-

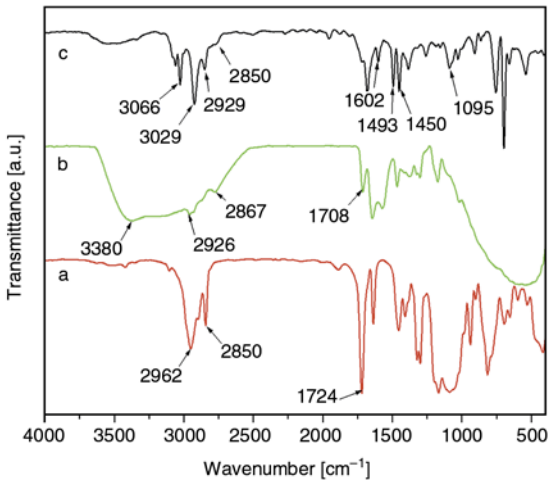

Figure 2. FTIR spectra of (a) pristine MPS, (b) MPS-TiO_2 and (c) TiO_2/PS composites

cessfully. The shift of the C=O vibration band from 1724 to 1708 cm^{-1} is due to the formation of the hydrogen bond between the carbonyl group from MPS and the hydroxyl groups on the surface of TiO_2. A similar phenomenon appeared in the previous spectra as well [33]. From Figure 2, it also displays the typical titanium broad absorption bands at about 450–800 cm^{-1} (Figure 2b). The typical PS absorption bands at 1450, 1493, 1602, 2929, and 3029 cm^{-1} are clearly seen in the spectrum of TiO_2/PS sol hybrids (Figure 2c).

The relative amounts of grafted MPS on TiO_2 and PS on MPS-TiO_2 were determined by TGA through the thermal decomposition of MPS and PS under argon atmosphere. As shown in Figure 3, for the MPS-TiO_2 particles, there are three main temperature regions of weight loss. The weight loss below 300°C can be attributed to the evaporation of physical absorbed water and residual solvent in the samples; the weight loss in the temperature region of 300–460°C can be resulted from the decomposition of MPS; the weight loss in the temperature beyond 460°C can be assigned to the decomposition of titania-bonded groups such as –OH [34]. For the TiO_2/PS core-shell particles, the decomposition temperature region of PS is observed at 350–460°C. According to the results, we can conclude that around 67% of residual for MPS-TiO_2 particles is left and around 19.9% for TiO_2/PS core-shell particulates. It is further confirmed that PS have been grafted to MPS-TiO_2 particles successfully, in accordance with the results of FT-IR.

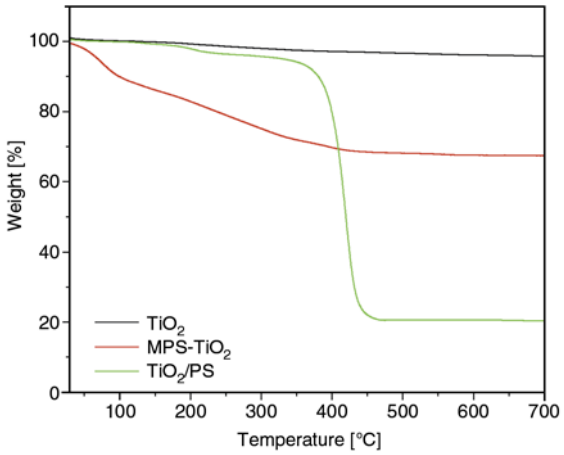

Figure 3. TGA curves of TiO_2, MPS-TiO_2 and TiO_2/PS core-shell particles

3.2. Surface morphology

Figure 4 shows a typical SEM image of PS (a), MPS-TiO_2 (b) and TiO_2/PS (c). From the SEM image of PS (Figure 4a), we can discover that the surface of the spheres is slippery, there is no hierarchical structure presented. For TiO_2 microspheres (Figure 4b), it can be found that the surface of MPS-TiO_2 microspheres with mean diameter of about 1 μm are very rough and seriously aggregated. However, the as-prepared TiO_2/PS microspheres are better dispersed and with larger mean diameter compared with MPS-TiO_2 (Figure 4c), originating from the facts that PS has been successfully grafted onto the surface of the as-prepared MPS-TiO_2 particles. In order to confirm the content of PS coating on the surface of MPS-TiO_2, the TiO_2/PS is also detected by the EDX. Figure 5 gives the EDX spectrum of the TiO_2/PS particulates. The element peaks of titanium together with little oxygen are very weak, confirming that MPS-TiO_2 is encapsulated by PS completely. There is a set of strong peaks in the graph, which belongs to carbon element. The peaks of Cu are for the copper foil, the appearance of this element may be the result of using copper foil as substrate to prepare TiO_2/PS coatings. It convincingly indicates that the

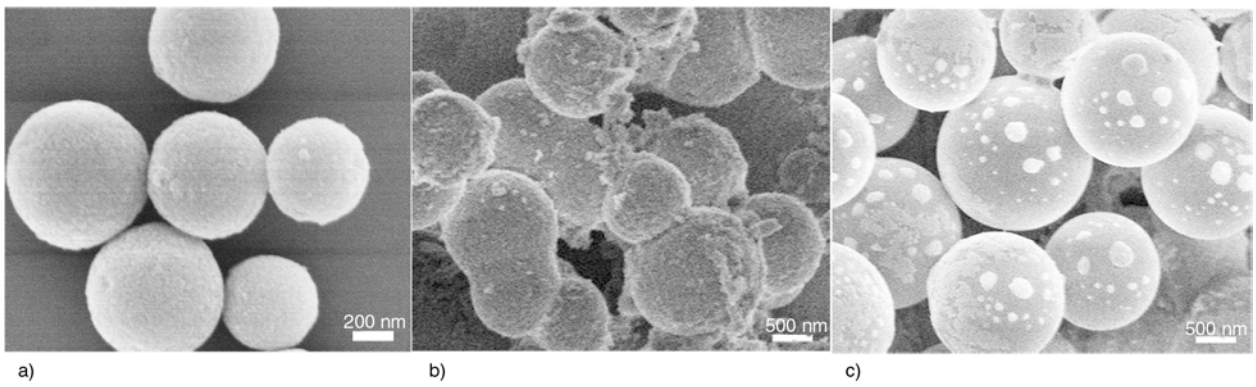

Figure 4. SEM images of PS (a), MPS-TiO_2 (b) and TiO_2/PS (c)

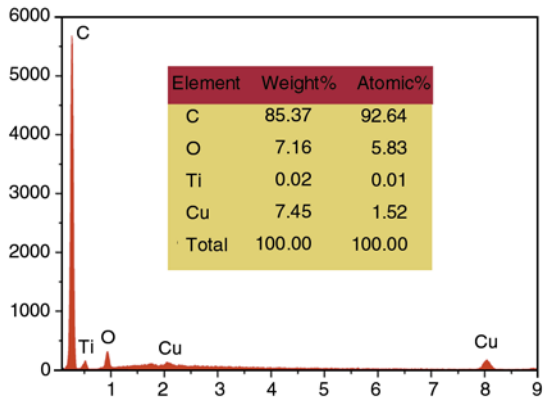

Figure 5. EDX spectrum of TiO_2/PS, the inset table is the elementary analysis for TiO_2/PS microspheres

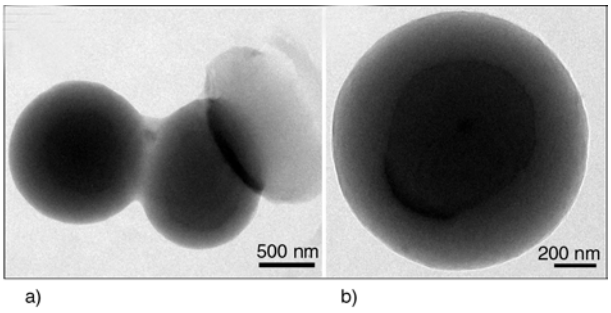

Figure 6. TEM images of TiO_2/PS core-shell particles with low (a) and high magnifications (b)

material coated on the surface of the MPS-TiO_2 is PS. The inset table is the elementary analysis for TiO_2/PS microspheres. It can be seen from the table that the carbon content on the surface of MPS-TiO_2 reaches 85.37 wt%, corresponding to the result of TGA measurement.

Figure 6 shows a typical transmission electron microscope (TEM) image of the as-prepared TiO_2/PS surface. It can be found that a well-defined core-shell structure with TiO_2 particles as core and PS as shell has been formed. The dispersed particles, which are regular in shape, have a distinct layer of PS chains grafted onto the surface of the titanium cores (Figure 6a). The magnification image clearly displays MPS-functionalized titanium cores with the diameter about 600 nm and the PS shell with the thickness about 200 nm (Figure 6b). The result coincides with our suggested mechanism.

3.3. Surface wettability

In the simplest case, the wettability of a solid surface is evaluated by the contact angle given by Young's equation. There exist three different phases when a drop of liquid is on a solid substrate. Generally, there are three surface tensions to consider: solid-liquid (γ_{SL}), liquid-vapor (γ_{LV}), and solid-vapor (γ_{SV}). The relationship between the cosine of the contact angle θ_y that the drop makes with the surface and the three surface tensions is given by Young's equation (Equation (1)):

$$\gamma_{SV} = \gamma_{SL} + \gamma_{LV} \cdot \cos\theta_y \quad (1)$$

Equation (1) can be interpreted as a mechanical force balance for the line of the three-phase contact and is always used under the condition of ideal surface.

As previously shown, surface wettability which depends on the surface energy is subject to Young's equation. However, this equation is not applicable to rough surfaces. The theory explaining such a transition from hydrophobicity to superhydrophobicity occurring on the rough surfaces was proposed by Wenzel [35]. According to Wenzel's modification of Young's equation, the roughness factor r enhances both hydrophilicity and hydrophobicity. The apparent contact angle θ_r is predicted by the following Equation (2):

$$\cos\theta_r = \frac{r \cdot (\gamma_{SV} - \gamma_{SL})}{\gamma_{LV}} = r \cdot \cos\theta \quad (2)$$

Here, r is the roughness of the surface, which is the ratio between the actual surface and its horizontal projection. θ_r and θ are the water CAs of a rough surface and a native flat surface, respectively. It is easy to deduce from Equation (2), when the intrinsic water contact angle is larger than 90° on a flat surface, the hydrophobicity of the surface is enhanced by this effect. In contrast, when the intrinsic water contact angle is smaller than 90° on a flat surface, the hydrophilicity of the surface is enhanced by this effect. Here, θ is 110±2°. Figure 7 shows the water CAs of PS (a), colloid MPS-TiO_2 gels (b) and TiO_2/PS particulates (c), the CAs of them are 94.5±1.5°, 110±2° and 153.5±1.5°, respectively. From Figure 4a we can find that the surface of PS spheres is slippery. When TiO_2 is modified by MPS for the first time, the surface of the TiO_2 is rough which can be seen from Figure 4b, resulting in the increase of θ_r. Then MPS-TiO_2 particles are encapsulated by PS, the surface presents hierarchical structure which also can be found from Figure 4c. The Wenzel mode can well explain why these surfaces are more hydrophobic after modification. In

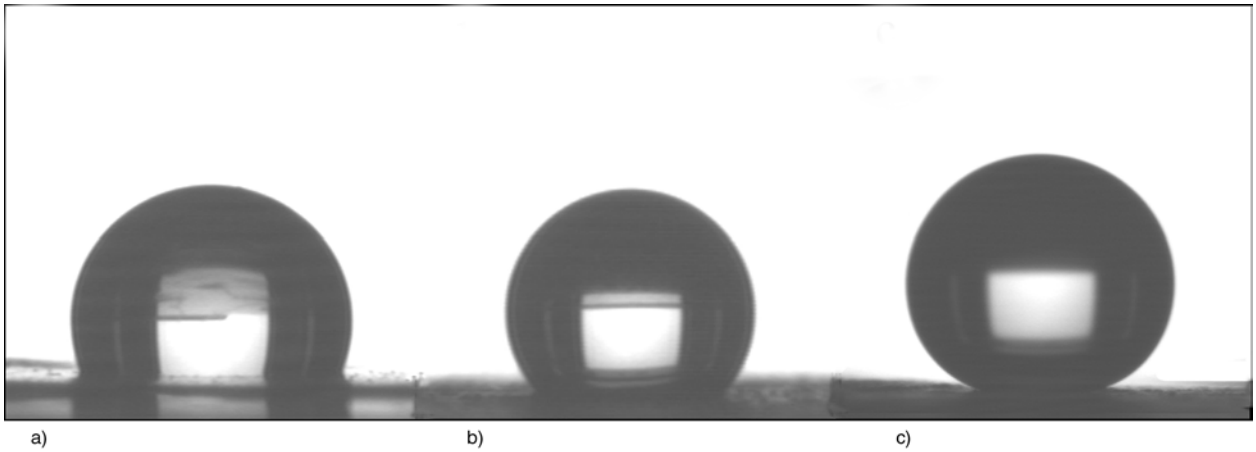

Figure 7. Images for the water CAs of PS (a), MPS-TiO_2 gels (b) and TiO_2/PS particulates (c)

the above cases, the hierarchical TiO_2/PS particulate surface has the biggest water CA after modification, which indicates that this hierarchical structure has the largest roughness. On the other hand, PS is a material of low surface energy, which may affect the hydrophobic property of the coatings. Figure 4c also presents that the 1 μm MPS-TiO_2 gels formed the micrometer structure, on the surface of which there are finer structures at the level of nanometer. The forming of this micro-/nanostructures structure can greatly improve the hydrophobicity of the TiO_2/PS coatings [30, 36].

Interestingly, the droplet deposited on the prepared surface is also featured by high adhesion and high hysteresis of the apparent contact angle. Water droplet on the studied surface keeps a spherical shape even when the surface is turned upside down, as shown in Figure 8. We find that the adhesive ability of the roughness TiO_2/PS-based surface is strong enough to catch a water droplet at a volume of 15 μl even when the copper foil substrate is tilted to 115° (Figure 8b) or turned upside down (Figure 8c), suggesting that the adhesion force between the as-prepared surface and the water droplet is larger than 150 μN. The strong adhesion between water and TiO_2/PS-based nanostructures can be explained mainly by the dispersive adhesion caused by van der Waals' forces, which are largely dependent on the distance between water droplets and surfaces, as confirmed in our experiments. It is significant that when the water droplets are getting close to the surface, the water is repelled and could hardly adhere to the surface until it eventually sticks to the surface. The van der Waals' mechanism of the gecko suggests that the remarkable adhesion property of the gecko's setae is mainly the result of the

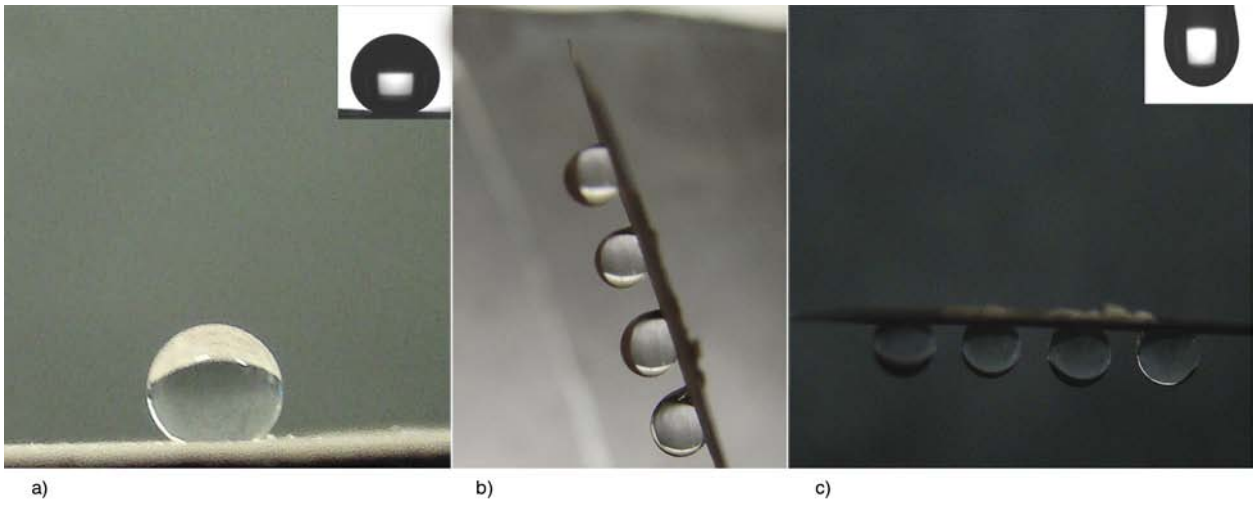

Figure 8. Shapes of water droplets on the as-prepared surface with different tilt angles: (a) 0°, (b) 115°, and (c) 180°. The inset of (a) is the water CA on the as-prepared surface with a value of about 153.5±1.5°. The weights of water droplets employed in (a–c) are about 10, 20, and 20 mg, respectively.

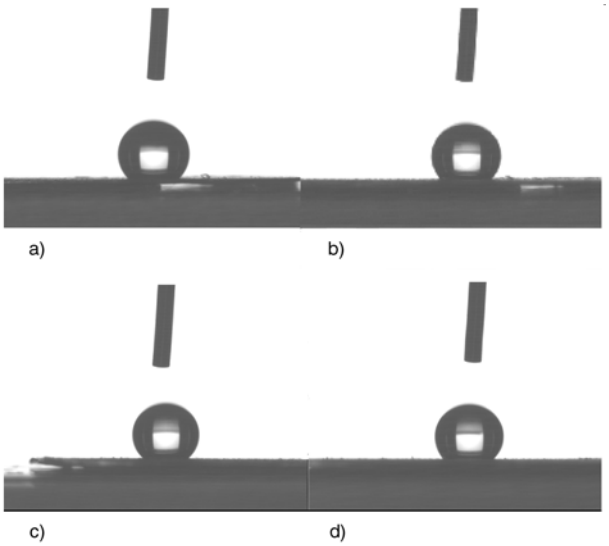

Figure 9. Photographs for the water CAs of TiO_2/PS coatings before and after being immersed in the ethanol (a, b) and exposed to UV light (c, d)

size and shape of its tips and is not strongly affected by chemical properties of the surface [37]. At the same time, according to the capillary mechanism, each micro-orifice produces a miniscule capillary force. Myriad micro-orifices and the wall roughness on the as-prepared surface acting together create formidable adhesion, which is sufficient to endure the weight of the water droplet even when the surface is turned upside down. The stability of the superhydrophobic film is tested by immersing the surfaces into water and ethanol solution overnight, it is found that the surface wetting property of the film did not change. Figure 9a and 9b present the water CAs of the films, they are 153±1° and 151.5±1° before and after being immersed in the ethanol. It also shows excellent optical stability for there is no change of the water CAs of the coatings when exposing to UV light after 30 minutes, which can be deduced from Figure 9, for the water CAs of TiO_2/PS coatings before and after exposing to UV light is 152±1° and 151±1°, respectively.

4. Conclusions

In conclusion, we have prepared a superhydrophobic TiO_2/PS surface with the biggest water contact angle of 153.5±1.5°. The raw materials of TiO_2 and styrene are pretty cheap, and the whole reaction involves two steps, which makes the synthetic process cost-effective and facile. Therefore, it is possible to apply it into industry applications. The as-prepared hybrids present excellent chemical and optical stability as well. Compared with the traditional superhydrophobic surfaces, the as-prepared surface shows a strong adhesive property. This novel wetting behavior is attributed to the distinct microscale surface roughness and heterogeneous surface composition. The highly surface roughness and hydrophobic component contribute to the high static CAs. These results offer us an opportunity to further understand the wettability of solid surface, and also could be used in important industrial applications. We anticipate that the prepared materials have many potential applications, for instance, in no loss microdroplet transfer, trace-liquid reactors, biochemical separation and *in-situ* detection.

Acknowledgements

Authors are thankful to Mr. Chengjun Pan, Mr. Li Zhou, Mr. Sijia Yan and Mr. Guoliang Wu for their kind help in preparing the manuscript. We are indebted to engineer Liu Zhen for TEM imaging.

References

[1] Schneider J. J.: Magnetic core/shell and quantum-confined semiconductor nanoparticles via chimie douce organometallic synthesis. Advanced Materials, **13**, 529–533 (2001).
DOI: 10.1002/1521-4095(200104)13:7<529::AID-ADMA529>3.0.CO;2-X

[2] Zhang K., Zheng L. L., Zhang X. H., Chen X., Yang B.: Silica-PMMA core-shell and hollow nanospheres. Colloids and Surfaces A: Physicochemical and Engineering Aspects, **277**, 145–150 (2006).
DOI: 10.1016/j.colsurfa.2005.11.049

[3] Landfester K., Rothe R., Antonietti M.: Convenient synthesis of fluorinated latexes and core-shell structures by miniemulsion polymerization. Macromolecules, **35**, 1658–1662 (2002).
DOI: 10.1021/ma011608a

[4] Kammona O., Kotti K., Kiparissides C., Celis J. P., Fransaer J.: Synthesis of polymeric and hybrid nanoparticles for electroplating applications. Electrochimica Acta, **54**, 2450–2457 (2009).
DOI: 10.1016/j.electacta.2008.05.017

[5] Chen X., Cui Z. C., Chen Z. M., Zhang K., Lu G., Zhang G., Yang B.: The synthesis and characterizations of monodisperse cross-linked polymer microspheres with carboxyl on the surface. Polymer, **43**, 4147–4152 (2002).
DOI: 10.1016/S0032-3861(02)00262-8

[6] Fu L. J., Liu H., Zhang H. P., Li C., Zhang T., Wu Y. P., Holze R., Wu H. Q.: Synthesis and electrochemical performance of novel core/shell structured nanocomposites. Electrochemistry Communications, **8**, 1–4 (2006).
DOI: 10.1016/j.elecom.2005.10.006

[7] Marinakos S. M., Brousseau L. C., Jones A., Feldheim D. L.: Template synthesis of one-dimensional Au, Au-poly(pyrrole), and poly(pyrrole) nanoparticle arrays. Chemistry of Materials, **10**, 1214–1219 (1998).
DOI: 10.1021/cm980059t

[8] Zhang K., Chen H. T., Chen X., Chen Z. M., Cui Z. C., Yang B.: Monodisperse silica-polymer core-shell microspheres via surface grafting and emulsion polymerization. Macromolecular Materials and Engineering, **288**, 380–385 (2003).
DOI: 10.1002/mame.200390031

[9] Kumaraswamy G., Dibaj A. M., Caruso F.: Photonic materials from self-assembly of 'tolerant' core-shell coated colloids. Langmuir, **18**, 4150–4154 (2002).
DOI: 10.1021/la011772r

[10] Song X. F., Gao L.: Fabrication of hollow hybrid microspheres coated with silica/titania via sol-gel process and enhanced photocatalytic activities. The Journal of Physical Chemistry C, **23**, 8180–8187 (2007).
DOI: 10.1021/jp071142j

[11] Lee K., Lyu S., Lee S., Kim Y. S., Hwang W.: Characteristics and self-cleaning effect of the transparent super-hydrophobic film having nanofibers array structures. Applied Surface Science, **256**, 6729–6735 (2010).
DOI: 10.1016/j.apsusc.2010.04.081

[12] Jin M. H., Feng X. J., Feng L., Sun T. L., Zhai J., Li T. J., Jiang L.: Superhydrophobic aligned polystyrene nanotube films with high adhesive force. Advanced Materials, **17**, 1977–1981 (2005).
DOI: 10.1002/adma.200401726

[13] Bormashenko E., Bormashenko Y., Stein T., Whyman G., Pogreb R., Barkay Z.: Environmental scanning electron microscopy study of the fine structure of the triple line and Cassie-Wenzel wetting transition for sessile drops deposited on rough polymer substrates. Langmuir, **23**, 4378–4382 (2007).
DOI: 10.1021/la0634802

[14] Feng X. J., Feng L., Jin M. H., Zhai J., Jiang L., Zhu D. B.: Reversible super-hydrophobicity to super-hydrophilicity transition of aligned ZnO nanorod films. Journal of the American Chemical Society, **126**, 62–63 (2004).
DOI: 10.1021/ja038636o

[15] Nimittrakoolchai O., Supothina S.: Polymer-based superhydrophobic coating fabricated from polyelectrolyte multilayers of poly(allylamine hydrochloride) and poly(acrylic acid). Macromolecular Symposia, **264**, 73–79 (2008).
DOI: 10.1002/masy.200850412

[16] Lim H. S., Han J. T., Kwak D. H., Jin M. H., Cho K.: Photoreversibly switchable superhydrophobic surface with erasable and rewritable pattern. Journal of the American Chemical Society, **128**, 14458–14459 (2006).
DOI: 10.1021/ja0655901

[17] Amigoni S., de Givenchy E. T., Dufay M., Guittard F.: Covalent layer-by-layer assembled superhydrophobic organic-inorganic hybrid films. Langmuir, **25**, 11073–11077 (2009).
DOI: 10.1021/la901369f

[18] Jin M. H., Feng X. J., Xi J. M., Zhai J., Cho K., Feng L., Jiang L.: Super-hydrophobic PDMS surface with ultra-low adhesive force. Macromolecular Rapid Communications, **26**, 1805–1809 (2005).
DOI: 10.1002/marc.200500458

[19] Chen W., Fadeev A. Y., Hsieh M. C., Öner D., Youngbloo J., McCarthy T. J.: Ultrahydrophobic and ultralyophobic surfaces: Some comments and examples. Langmuir, **15**, 3395–3399 (1999).
DOI: 10.1021/la990074s

[20] Guo Z. G., Fang J., Hao J. C., Liang Y. M., Liu W. M.: A novel approach to stable superhydrophobic surfaces. ChemPhysChem, **7**, 1674–1677 (2006).
DOI: 10.1002/cphc.200600217

[21] Hikita M., Tanaka K., Nakamura T., Kajiyama T., Takahara A.: Super-liquid-repellent surfaces prepared by colloidal silica nanoparticles covered with fluoroalkyl groups. Langmuir, **21**, 7299–7302 (2005).
DOI: 10.1021/la050901r

[22] Tadanaga K., Morinaga J., Matsuda A., Minami T.: Superhydrophobic-superhydrophilic micropatterning on flowerlike alumina coating film by the sol-gel method. Chemistry of Materials, **12**, 590–592 (2000).
DOI: 10.1021/cm990643h

[23] Yang S. Y., Chen S., Tian Y., Feng C., Chen L.: Facile transformation of a native polystyrene (ps) film into a stable superhydrophobic surface via sol-gel process. Chemistry of Materials, **20**, 1233–1235 (2008).
DOI: 10.1021/cm703220r

[24] Peng Y. T., Lo K. F., Juang Y. J.: Constructing a superhydrophobic surface on polydimethylsiloxane via spin coating and vapor-liquid sol-gel process. Langmuir, **26**, 5167–5171 (2010).
DOI: 10.1021/la903646h

[25] Latthe S. S., Imai H., Ganesan V., Rao A. V.: Superhydrophobic silica films by sol-gel co-precursor method. Applied Surface Science, **256**, 217–222 (2009).
DOI: 10.1016/j.apsusc.2009.07.113

[26] Du X., Liu X. M., Chen H. M., He J. H.: Facile fabrication of raspberry-like composite nanoparticles and their application as building blocks for constructing superhydrophilic coatings. The Journal of Physical Chemistry C, **113**, 9063–9070 (2009).
DOI: 10.1021/jp9016344

[27] Alivisatos A. P.: Semiconductor clusters, nanocrystals, and quantum dots. Science, **271**, 933–937 (1996).
DOI: 10.1126/science.271.5251.933

[28] Yang J., Zhang Z. Z., Men X. H., Xu X. H., Zhu X. T.: Reversible conversion of water-droplet mobility from rollable to pinned on a superhydrophobic functionalized carbon nanotube film. Journal of Colloid and Interface Science, **346**, 241–247 (2010).
DOI: 10.1016/j.jcis.2010.02.040

[29] Nakajima A., Fujishima A., Hashimoto K., Watanabe T.: Preparation of transparent superhydrophobic boehmite and silica films by sublimation of aluminum acetylacetonate. Advanced Materials, **11**, 1365–1368 (1999).
DOI: 10.1002/(SICI)1521-4095(199911)11:16<1365::AID-ADMA1365>3.0.CO;2-F

[30] Peng J. Y., Yu P. R., Zeng S. J., Liu X., Chen J. R., Xu W. J.: Application of click chemistry in the fabrication of cactus-like hierarchical particulates for sticky superhydrophobic surfaces. The Journal of Physical Chemistry C, **114**, 5926–5931 (2010).
DOI: 10.1021/jp909430z

[31] Cheng Z. J., Feng L., Jiang L.: Tunable adhesive superhydrophobic surfaces for superparamagnetic microdroplets. Advanced Functional Materials, **18**, 3219–3225 (2008).
DOI: 10.1002/adfm.200800481

[32] Song X. Y., Zhai J., Wang Y. L., Jiang L.: Fabrication of superhydrophobic surfaces by self-assembly and their water-adhesion properties. The Journal of Physical Chemistry C, **109**, 4048–4052 (2005).
DOI: 10.1021/jp045152l

[33] Rong Y., Chen H. Z., Wu G., Wang M.: Preparation and characterization of titanium dioxide nanoparticle/polystyrene composites via radical polymerization. Materials Chemistry and Physics, **91**, 370–374 (2005).
DOI: 10.1016/j.matchemphys.2004.11.042

[34] Peng B., Tang F. Q., Chen D., Ren X. L., Meng X. W., Ren J.: Preparation of PS/TiO_2/UF multilayer core-shell hybrid microspheres with high stability. Journal of Colloid and Interface Science, **329**, 62–66 (2009).
DOI: 10.1016/j.jcis.2008.09.069

[35] Wenzel R. N.: Surface roughness and contact angle. The Journal of Physical Chemistry C, **53**, 1466–1467 (1949).
DOI: 10.1021/j150474a015

[36] Feng J., Huang M. D., Qian X.: Fabrication of polyethylene superhydrophobic surfaces by stretching-controlled micromolding. Macromolecular Materials and Engineering, **294**, 295–300 (2009).
DOI: 10.1002/mame.200800331

[37] Autumn K., Gravish N.: Gecko adhesion: Evolutionary nanotechnology. Philosophical Transactions of the Royal Society A, **366**, 1575–1590 (2008).
DOI: 10.1098/rsta.2007.2173